Research Paper

Nicotinamide nucleotide transhydrogenase (NNT) regulates mitochondrial ROS and endothelial dysfunction in response to angiotensin II

K.N. Shashanka Rao, Xinggui Shen, Sibile Pardue, David M. Krzywanski[*]

Department of Cellular Biology and Anatomy, School of Medicine, Center for Cardiovascular Diseases and Sciences, Louisiana State University Health Sciences Center – Shreveport, Shreveport, LA, 71103, United States

A B S T R A C T

Endothelial dysfunction is a critical, initiating step in the development of hypertension (HTN) and mitochondrial reactive oxygen species (ROS) are important contributors to endothelial dysfunction. Genome-wide association studies (GWAS) have identified single nucleotide polymorphisms (SNPs) in the nicotinamide nucleotide trans-hydrogenase (*Nnt*) gene that are associated with endothelial dysfunction and increased risk for HTN. NNT is emerging as an important enzyme that regulates mitochondrial NADPH levels and mitochondrial redox balance by supporting the thiol dependent peroxidase systems in the mitochondria. We have previously shown that the absence of NNT in C57Bl/6J animals promotes a more severe hypertensive phenotype through reductions in $^{\bullet}$NO and endothelial dependent vessel dilation. However, the impact of NNT on human endothelial cell function remains unclear. We utilized NNT directed shRNA in human aortic endothelial cells to test the hypothesis that NNT critically regulates mitochondrial redox balance and endothelial function in response to angiotensin II (Ang II). We demonstrate that NNT expression and activity are elevated in response to the mitochondrial dysfunction and oxidative stress associated with Ang II treatment. Knockdown of NNT led to a significant elevation of mitochondrial ROS production and impaired glutathione peroxidase and glutathione reductase activities associated with a reduction in the NADPH/NADP$^+$ ratio. Loss of NNT also promoted mitochondrial dysfunction, disruption of the mitochondrial membrane potential, and impaired ATP production in response to Ang II. Finally, we observed that, while the loss of NNT augmented eNOS phosphorylation at Ser^{1177}, neither eNOS activity nor nitric oxide production were similarly increased. The results from these studies clearly demonstrate that NNT is critical for the maintenance of mitochondrial redox balance and mitochondrial function. Loss of NNT and disruption of redox balance leads to oxidative stress that compromises eNOS activity that could have a profound effect on the endothelium dependent regulation of vascular tone.

1. Introduction

Hypertension (HTN) remains a significant health concern in the United States with approximately 30% of all individuals over the age of 20 diagnosed with HTN with an annual health care cost of $42.9 billion [1]. Despite multiple therapeutic options, only half of these patients have their blood pressure under control and the prevalence of treatment resistant HTN has increased from 8.9% in 2008 to 19.7% (10.3 million adults) in 2018 [2]. Reactive oxygen species (ROS) plays a critical role in the pathogenesis of HTN by contributing to changes in vascular tone and structure that lead to increased peripheral resistance and pressure [3]. While the NADPH oxidase family of enzymes are a critical source of ROS [3], mounting evidence indicates that mitochondrial-derived ROS may play an equally important role in HTN [4]. Mitochondrial ROS generation occurs during oxidative phosphorylation, where ~4-5% of total oxygen consumption during this process leads to the formation of superoxide ($O_2^{\bullet-}$) [5,6] and hydrogen peroxide (H_2O_2) via a direct two-electron reduction of molecular oxygen. Elevated levels of ROS can negatively impact the regulation of blood pressure by contributing to endothelial dysfunction [7] and through the removal of bioavailable nitric oxide [8] ($^{\bullet}$NO). Furthermore, chronic elevations in ROS can stimulate vascular remodeling leading to reduced lumen diameter and increased intimal thickening that impair vessel plasticity. Ultimately, these structural and functional changes in the vasculature lead to

increased vascular pressure and risk for a cardiovascular event [9].

Mitochondrial $O_2^{\bullet-}$, and the product of its dismutation, H_2O_2, play critical roles in the development of HTN [10]. Furthermore, increased levels of $O_2^{\bullet-}$ and H_2O_2 have been observed in plasma and tissues from hypertensive patients [11,12]. Mitochondrial ROS mediate changes in pressure in a number of ways, the most evident being the disruption of $^{\bullet}$NO dependent vessel dilation. The loss of bioavailable $^{\bullet}$NO is associated with endothelial dysfunction in a number of cardiovascular diseases [13], including HTN [14–17]. These data are consistent with the ability of $^{\bullet}$NO to be rapidly consumed by reaction with $O_2^{\bullet-}$ leading to the formation peroxynitrite ($ONOO^-$) that can contribute to mitochondrial and endothelial dysfunction via eNOS uncoupling and further generation of $O_2^{\bullet-}$ [18]. Mitochondria possess multiple antioxidant systems that function to maintain the balance between ROS production and consumption. In the mitochondrial matrix, $O_2^{\bullet-}$ is efficiently converted to H_2O_2 by the activity of manganese superoxide dismutase (MnSOD) [19–21]. H_2O_2 is further detoxified to water by multiple thiol-dependent reductive pathways in the mitochondria that include the peoxiredoxin, thioredoxin, thioredoxin reductase system and the glutathione peroxidase, glutathione, glutathione reductase system. Interestingly, all of the antioxidant systems downstream of MnSOD in the mitochondria are either directly or indirectly dependent on NADPH to provide the reducing equivalents to maintain mitochondrial redox balance.

Mitochondria possess several enzymatic sources of NADPH including nicotinamide nucleotide transhydrogenase (NNT), NADP-dependent isocitrate dehydrogenase, NADPH-dependent malic enzyme, and glutamate dehydrogenase [22–27]. NNT is a ubiquitous mitochondrial inner membrane protein that couples proton translocation across the mitochondrial inner membrane to a redox reaction that reduces mitochondrial $NADP^+$ while oxidizing NADH [28–30]. Genome-wide association studies (GWAS) have identified several single nucleotide polymorphisms (SNPs) in the nicotinamide nucleotide transhydrogenase (*Nnt*) gene that are associated with endothelial dysfunction and increased risk for HTN [31,32]. In HTN, substitution of an A allele for a G allele at base pair 43824677 on chromosome 5 was associated with decreased NNT expression and increased blood pressure [31]. The contribution of NNT to cardiometabolic disease has primarily been studied in the C57Bl/6N and C57Bl/6J mice where a deletion mutation leads to the loss of NNT expression and activity in 6J mice [33,34]. In 6J mice, the loss of NNT leads increased mitochondrial H_2O_2 production and a reduced GSH/GSSG ratio compared to the 6N animals [35]. Although some studies have observed that the absence of NNT in 6J mice had no impact on glucose tolerance [36,37] or protected against heart failure [38], the prevailing literature implicates the loss of NNT in increased cardiovascular disease susceptibility. 6J mice display symptoms of glucose intolerance [39] and are highly susceptible to the development of obesity, insulin resistance, and type-2 diabetes when placed on high fat diet [40,41]. Furthermore, we have demonstrated that 6J mice develop a more severe hypertensive phenotype compared to 6N when treated with Ang II [42]. However, NNT's impact on mitochondrial and endothelial function in human vascular cell function remains completely undefined. We utilized NNT directed shRNA in human aortic endothelial cells to test the hypothesis that NNT critically regulates mitochondrial redox balance and endothelial function in response to Ang II. We demonstrate that the loss of NNT results in increased production of mitochondrial ROS, promotes mitochondrial dysfunction, and disrupts eNOS activity that is consistent with endothelial dysfunction that is a hallmark of HTN.

2. Materials and methods

2.1. Chemicals and reagents

All chemicals were at least analytical grade and purchased from Sigma Chemical Co., St. Louis, MO unless otherwise noted.

2.2. Cell culture and shRNA knockdown of NNT in human aortic endothelial cells

Immortalized human aortic endothelial cells (HAECs) were developed by transfection with a transgene containing the doxycycline-sensitive SV-40 large T-antigen. Immunoblotting of the resultant cell line indicated that large T-antigen was only expressed in the presence of doxycycline. Cells were maintained in MCDB 131 medium supplemented with 10% FBS, 2 mmol/L glutamax, 10 U/mL penicillin (GIBCO/Life technologies, Carlsbad, CA), 100 μg/mL streptomycin (GIBCO/Life technologies, Carlsbad, CA), 30 μg/mL heparin sodium, bovine brain extract (25 μg/mL), and doxycycline (40 μg/ml). Small hairpin RNA knockdown of NNT was accomplished by infecting immortalized HAECs at 30-50% confluency with 1.5×10^6 lentiviral particles containing either EGFP-scrambled (non-targeted) shRNA or EGFP-shNNT targeted shRNA (5′- CGAGAAGCTAATAGCATTATT-3′) (Vector Labs) according to the manufacturer's instructions. Virally transduced cells were sorted by fluorescence-activated cell sorting, resulting in paired cell lines of HAECs either possessing (Scr) or lacking (shNNT) *Nnt*. Expression of NNT was verified by Western blot. Doxycycline is removed from the media one passage prior to experimentation to turn off the expression of large T-antigen.

2.3. Isolation of endothelial mitochondria

Endothelial mitochondria were isolated for the NNT activity assay and other measurements according to the following protocol. HAECs were grown in 10 cm dishes and until they reached 80-90% confluency. Growth media was replaced with reduced-serum (0.5% serum) culture media for 16 h. The following day, HAEC, Scr, or shNNT cells were treated with vehicle or angiotensin II (500 nM) in serum-free medium for the times indicated. All the following steps were performed at 4 °C unless otherwise noted. Following treatment, cells were collected in ice-cold PBS and centrifuged for 5 min at 1600 rpm. The supernatant was discarded, and the cell pellets were flash frozen with liquid nitrogen. The cells were resuspended in 2 ml of $2.5\times$ RSB hypotonic buffer (10 mM NaCl, 1.5 mM $MgCl_2$, 10 mM Tris-HCl, pH 7.5) and incubated for 5 min on ice. Cells were homogenized with 50 strokes of Dounce homogenizer on ice. 1.35 ml of $2.5\times$ MS buffer (525 mM mannitol, 175 mM sucrose, 12.5 mM Tris-HCl, 2.5 mM EDTA, pH 7.5) was added to the samples and they were centrifuged at $1000\times g$ for 5 min. The supernatant was transferred to clean tube and spun at $12000\times g$ for 5 min and the supernatant was discarded. The mitochondrial pellet was washed in $1\times$ RSB hypotonic buffer (210 mM mannitol, 70 mM sucrose, 5 mM Tris-HCl, 1 mM EDTA, pH 7.5) and spun at $12000\times g$ for 5 min. The supernatant was discarded, and the clean mitochondrial pellet was used for further measurements.

2.4. Measurement of NNT activity

The activity of NNT was measured as previously described [43,44], with minor modifications. Briefly, the changes in differential absorbance (375–425 nm) due to the reduction of 3-acetylpyridine adenine dinucleotide (APAD), which is a NAD^+ analogue, were monitored for 5 min at 37 °C in a dual wavelength spectrophotometer. The assay medium contained 50 mM Tris (pH 8.0), 0.5% Brij-35, 1 mg/ml lysolecithin, 300 μM APAD, and 10 mg of mitochondrial protein; the reaction was initiated with 300 μM NADPH after 5 min preincubation. The slopes of absorbance over time were converted to nmol APAD reduced/min using the molar extinction coefficient of 5.1 $mM^{-1} \times cm^{-1}$ for reduced APAD [43]. Data are expressed as percent control (untreated cells).

2.5. Determination of mitochondrial bioenergetic profile

A Seahorse Bioscience XF24 extracellular flux analyzer was used to measure mitochondrial function in HAECs. The XF24 creates a transient,

7-μL chamber in specialized microplates that allows for the determination of oxygen and proton concentrations in real time [45,46]. Thus, the rates of oxygen consumption and proton production can be measured across several samples at a time. Measurements of extracellular flux were made in unbuffered media. For these experiments, cells were seeded at 40,000 cells per well onto Seahorse Bioscience (North Billerica, MA) V7 tissue culture plates in reduced-serum (0.5% serum) culture media and allowed to adhere and grow for 16 h. The following day, Scr and shNNT cells were treated with vehicle or angiotensin II (500 nM) using serum-free medium for 2 h. One hour before the start of the extracellular flux assay the media was changed to serum-free DMEM supplemented with 25 mmol/L D-glucose, 2 mmol/L L-glutamine, and 1 mmol/L pyruvate. The pH of the medium was adjusted to 7.4 with NaOH. To allow comparison between experiments, data are expressed as the rate of oxygen consumption in pmol/min/μg protein. To assay mitochondrial function, oligomycin, carbonyl cyanide-4-(trifluoromethoxy)phenylhydrazone, and a combination of antimycin A/rotenone were injected through ports in the Seahorse Flux Pak cartridges to final concentrations of 1 μg/mL, 1 μmol/L, and 10 μmol/L/1 μmol/L, respectively. Baseline oxygen consumption rate (OCR) is represented by the total OCR of the cells before addition of mitochondrial inhibitors. Because oligomycin inhibits mitochondrial ATP synthase (complex V), non-ATP–linked OCR is equal to the rate observed in the presence of oligomycin (OCR_{oligo}). Consequently, ATP-linked OCR (OCR_{ATP}) is determined by subtracting the non-ATP OCR from the baseline OCR ($OCR_{ATP}=OCR_{baseline}-OCR_{oligo}$). Maximal OCR ($OCR_{max}$) is determined in the presence of carbonyl cyanide-4-(trifluoromethoxy) phenylhydrazone, an ionophore that uncouples the mitochondrion, leading to maximal oxygen consumption in an attempt to re-establish a membrane potential. Finally, addition of antimycin A and rotenone blocks electron entry into the electron transport chain, inhibiting mitochondrial oxygen consumption, which allows estimation of nonmitochondrial OCR.

2.6. Measurement of reactive oxygen species

Cells were plated in 6-well dishes and allowed to reach confluence. The cells were then placed in a reduced-serum environment (0.5% serum) for 16 h and experiments were conducted using serum and phenol red-free medium. Endothelial superoxide production was measured using the hydroethidine (HE) reverse-phase high-performance liquid chromatography (HPLC) method, as previously reported [47]. Briefly, Scr and shNNT cells were treated with vehicle or angiotensin II (500 nM) for various times and then incubated with cell culture medium containing 10 μM HE for 30 min. Cells were then washed with PBS, pelleted, and lysed with a Triton X-100 solution. Proteins in the solution were precipitated using acidified methanol and 2-OH-ethidium (2-OH-E$^+$) enriched using a microcolumn preparation of Dowex 50WX-8 cation exchange resin and eluted with 10 N HCl. 2-OH-E$^+$ product was measured using fluorescence detection (excitation 490 nm; emission 567 nm) with a Shimadzu HPLC system (Shimadzu Corporation). 2-OH-E$^+$ concentration was normalized to total protein. Peaks for both the parent HE and (2-OH-E$^+$) were detected in all HPLC runs ensuring that the HE was not exhausted during superoxide detection. Hydrogen peroxide was measured using the ROS-Glo H_2O_2 assay (Promega) according to the manufacturer's instructions. Briefly, Scr and shNNT cells (1×10^4 cells/100 μL) were seeded into each well of a 96-well plate. Cells were incubated with or without angiotensin II (500 nM) and H_2O_2 substrate solution for the times indicated, followed by the addition of the ROS-Glo detection solution. Luminescence was measured using the CLARIOstar Plus plate reader (BMG Labtech). All the values were normalized to protein concentrations.

2.7. Determination of NADPH/NADP$^+$ and NADH/NAD$^+$ levels

NADPH/NADP$^+$ and NADH/NAD$^+$ ratios were determined using the NADP/NADPH-Glo and NAD/NADH-Glo assay kits (Promega) according to the manufacturer's instructions. Scr and shNNT cells were (1×10^4 cells/100 μL) were seeded into each well of a 96-well plate. The cells were then placed in a reduced-serum environment (0.5% serum) for 16 h and experiments were conducted using serum and phenol red-free medium. Cells were then treated with angiotensin II (500 nM) for the times indicated. NADPH/NADP$^+$ and NADH/NAD$^+$ were determined in independent experiments. Cells were lysed in 0.2 m NaOH, 1% (w/v) dodecyltrimethylammonium bromide followed by treatment with 0.4 m HCl at 60 °C for 15 min. After neutralization with 0.5 m Tris base, samples were then mixed with an equal volume of NADP/NADPH-Glo or NAD/NADH-Glo detection reagent (Promega) prepared immediately before use. Luciferin luminescence was measured continuously for 2 h using the CLARIOstar Plus plate reader (BMG Labtech). The slope of the luciferin signal from the linear range of the assay was used to determine relative NADPH/NADP$^+$ and NADH/NAD$^+$ concentration compared with a Scr control.

2.8. Mitochondrial glutathione peroxidase and glutathione reductase activity

Glutathione peroxidase activity was assayed using Cayman's Glutathione peroxidase Assay Kit (Cat. No. 706002) and glutathione reductase activity was determined using Cayman's glutathione reductase Assay Kit (Cat. No. 703202). Isolated mitochondria were prepared as described above and enzyme activities were determined in mitochondrial lysates according to the manufacturer's instructions. Activity was measured using the CLARIOstar Plus plate reader (BMG Labtech). All the values were normalized to protein concentrations.

2.9. Mitochondrial ATP levels

Mitochondrial ATP levels were assayed using Cayman's ATP Detection Assay Kit (Cat. No. 700410). Isolated mitochondria were prepared as described above and ATP levels were determined in mitochondrial lysates according to the manufacturer's instructions. Luminescence was measured using the CLARIOstar Plus plate reader (BMG Labtech). Micromolar concentrations were determined by comparison to an ATP standard curve.

2.10. Western blot analysis

Scr and shNNT endothelial cells were lysed in Pierce® MPER lysis buffer containing 1× protease inhibitor cocktail (Thermo Scientific)and 1× phosphatase inhibitor cocktail (Sigma Aldrich). Protein concentration of endothelial cells was determined by BioRad Protein Assay Kit. 20 μg of total protein for each sample was loaded onto a 10% SDS polyacrylamide gel. Proteins were separated at 120V for 120 min and protein transfer was performed for 120 min at 75 V onto a polyvinylidene difluoride (Immobilon-FL) membrane (EMD Millipore). The membranes were blocked for 1 h at room temperature in 5% non-fat dry milk (NFDM) in 1× phosphate buffered saline (PBS). Primary antibodies were diluted 1:1,000 in 5% NFDM in PBS, excluding β-actin which was diluted 1:5,000, and were incubated on the membranes overnight at 4 °C on a rocker.

Secondary antibodies were diluted 1:2,000 in 5% milk with Tris-buffered saline with 0.1% Tween 20 (TBST), excluding the β-actin secondary antibody which was diluted 1:10,000, and incubated with membranes for 2 h at room temperature. The membranes were washed three 3 times, for 15 min each, with TBST while rocking after incubation with both primary and secondary antibodies. BioRad Clarity Western blotting reagent (BioRad, 705060) was mixed and added to blots for 5 min. Images were acquired with the BioRad ChemiDoc Imaging System. Densitometry was performed using Image J analysis software. Bands of interest were normalized to β-actin or total eNOS for statistical analysis. Primary antibodies were as follows: NNT (sc-390236) (purchased from Santa Cruz), P-eNOS Ser^{1177} (C9C3 #9570), total eNOS (D9A5L #32027), and β-actin (8H10D10 #3700) (all purchased from Cell

Signaling), Secondary antibodies were as follows: anti-rabbit IgG-HRP (#7074) and anti-mouse IgG-HRP (#7076) (purchased from Cell Signaling).

2.11. Mitochondrial membrane potential

Scr and shNNT cells were grown to confluence in 4-well chambered slides. The cells were then placed in a reduced-serum environment (0.5% serum) for 16 h and experiments were conducted using serum and phenol red-free medium. Cells were treated with vehicle control or angiotensin II (500 nM) for the times indicated. Membrane potential was assessed using the potentiometric dye tetramethyl rhodamine methyl ester (TMRM; Sigma Aldrich) at a final concentration of 50 nM for 30 min at 37 °C. Four randomly selected images were acquired for each experimental replicate and digitized using a Hamamatsu Orca digital camera interfaced with an Olympus IX-70 microscope equipped for epifluorescent illumination. The camera signal was ported to an Apple Macintosh computer hosting the imaging software I Vision-MAC (Bio-vision, Exton, PA). Image analysis was performed using Image J analysis software.

2.12. Endothelial nitric oxide synthase (eNOS) activity

Endothelial nitric oxide synthase (eNOS) activity was assayed using Cayman's NOS Activity Assay Kit (Cat. No. 781001) according to the manufacturer's instructions. Activity was measured using the CLAR-IOstar Plus plate reader (BMG Labtech). All the values were normalized to protein concentrations.

2.13. NO measurements

Nitric oxide ($^\bullet$NO) metabolites (NOx) were measured using Sievers Nitric Oxide Analyzer 280i as previously described [48]. Following treatment cells were collected in $^\bullet$NO preservation solution (800 mmol/L potassium ferricyanide, 17.6 mmol/L N-ethylmaleimide, 6% Nonidet P-40 in PBS) for tri-iodide $^\bullet$NO chemiluminescent analysis. Nitrite is reduced using the tri-iodide method. $^\bullet$NO is measured using an ozone-based chemiluminescent assay (Sievers Nitric Oxide Analyzer 280i, Weddington, NC). Aliquots of samples were tested for sulfanil-amide resistance following addition of an acidic sulfanilamide solution to a final concentration of 0.5% v/v and sitting in the dark for 15 min prior to injection into the analyzer.

2.14. Statistical analysis

All of the studies have been repeated at least 3 times. Student's *t*-test was used for two-group comparison, and one-way ANOVA followed by the Newman–Keuls posttest was used for multigroup comparisons. Data were reported as mean $\pm$ SEM. $P < 0.05$ was considered significant.

3. Results

3.1. Angiotensin II induces mitochondrial dysfunction and NNT activity

Previous studies performed by our group and others has demonstrated that the absence of nicotinamide nucleotide transhydrogenase (NNT) exacerbates cardiovascular disease development in C57Bl/6J (6J) mice when compared to C57Bl/6N (6N) by contributing to mitochondrial dysfunction and increased ROS production [33,34,39–42,49]. However, the vast majority of these studies have been conducted in the 6N and 6J mice or cells derived from them. As such, very little is known regarding the regulation of NNT and its contribution to redox balance and mitochondrial function in human vascular cells. Consistent with previous reports, we observe a significant impairment of mitochondrial function in response to angiotensin II (Ang II) in human aortic endo-thelial cells (HAEC) highlighted by decreases in basal, oligomycin

(ATP-linked), and FCCP (maximal oxygen consumption) treated conditions (Fig. 1A). The mitochondrial dysfunction incited by Ang II treatment led to significant oxidative stress exemplified by corresponding increases in both superoxide (Fig. 1B) and hydrogen peroxide (Fig. 1C) production in response to treatment. NNT is located in the mitochondrial inner membrane and utilizes the mitochondrial membrane potential to convert NADH to NADPH [28–30]. As such, it plays a pivotal role in supplying the NADPH that is utilized by the antioxidant systems in the mitochondria including glutathione peroxidase (Gpx), and glutathione reductase (GR) which have critical roles in the removal of hydrogen peroxide and the maintenance of reduced GSH respectively. In response to Ang II treatment we observe a time dependent increase in both the expression and activity of NNT (Fig. 1D) consistent with a role in preventing ROS-induced damage and dysfunction.

3.2. NNT supports mitochondrial antioxidant activity

To determine if NNT plays a significant role in the ability of mitochondria to cope with Ang II-induced oxidative stress, we utilized a small hairpin RNA (shRNA) strategy to knockdown NNT expression in HAECs. Fig. 2A demonstrates that shRNA treatment led to an almost complete inhibition of NNT expression and activity in these cells. NNT's role in supplying the mitochondrial antioxidant systems with reducing equivalents in the form of NADPH would suggest that the loss of NNT could contribute to a pro-oxidative redox environment in the mitochondria. Supporting this concept, we observe that the loss of NNT leads to an increase in both superoxide (Fig. 2B) and hydrogen peroxide (Fig. 2C) that is exacerbated by Ang II treatment. This shift in redox tone is likely driven by a disruption of NADH and NADPH balance in the mitochondria due to the loss of NNT in these cells. Consistent with this hypothesis, we observe that even in untreated conditions the loss of NNT led a significant decrease in NADPH levels (Fig. 2D) and a significant increase in NAD^+ (Fig. 2E). Treatment with Ang II exacerbated the loss of NADPH in these cells but did not further increase NAD^+. The loss of NADPH is likely due directly to the loss of NNT activity and augmented by consumption of NADPH via mitochondrial antioxidant enzyme activity. This concept is supported by data demonstrating that the loss of NNT in these cells has a significant impact on both glutathione peroxidase (Gpx) and glutathione reductase (GR) activities. The absence of NNT significantly increased both GR and Gpx activities in untreated HAEC (Fig. 2F and G), consistent with an increased steady-state H_2O_2 levels driven by the loss of NNT. However, treatment with Ang II and a further increase in H_2O_2 production (Fig. 2C) quickly overwhelms the diminished antioxidant capacity of the cells lacking NNT ultimately leading to a significant impairment of both enzyme activities. In contrast, cells that maintain normal NNT activity respond to Ang II and the increased H_2O_2 production with significant elevations of both Gpx and GR activities.

3.3. The loss of NNT contributes to mitochondrial dysfunction

Ang II treatment contributes to mitochondrial dysfunction in normal HAEC (Fig. 1A), however it is unclear what role NNT may play in this process. Interestingly, simply removing NNT from the cell results in an impairment of mitochondrial oxygen consumption under both basal and FCCP stimulated (maximal oxygen consumption) conditions (Fig. 3A) that is similar to the mitochondrial dysfunction we observe in HAEC treated with scrambled shRNA and Ang II (Fig. 3B). Treating cells that lack NNT with Ang II leads to further impairment of both basal and FCCP stimulated oxygen consumption in these cells that is more severe than both untreated shNNT cells (Fig. 3C) and cells treated with scrambled shRNA and Ang II (Fig. 3D). Summary data in Fig. 3E highlights that the loss NNT from these cells leads to a mitochondrial dysfunction similar to that observed with Ang II treatment alone and that Ang II treatment in the absence of NNT leads to a profound impairment of mitochondrial function. The mitochondrial dysfunction incited by the loss of NNT may
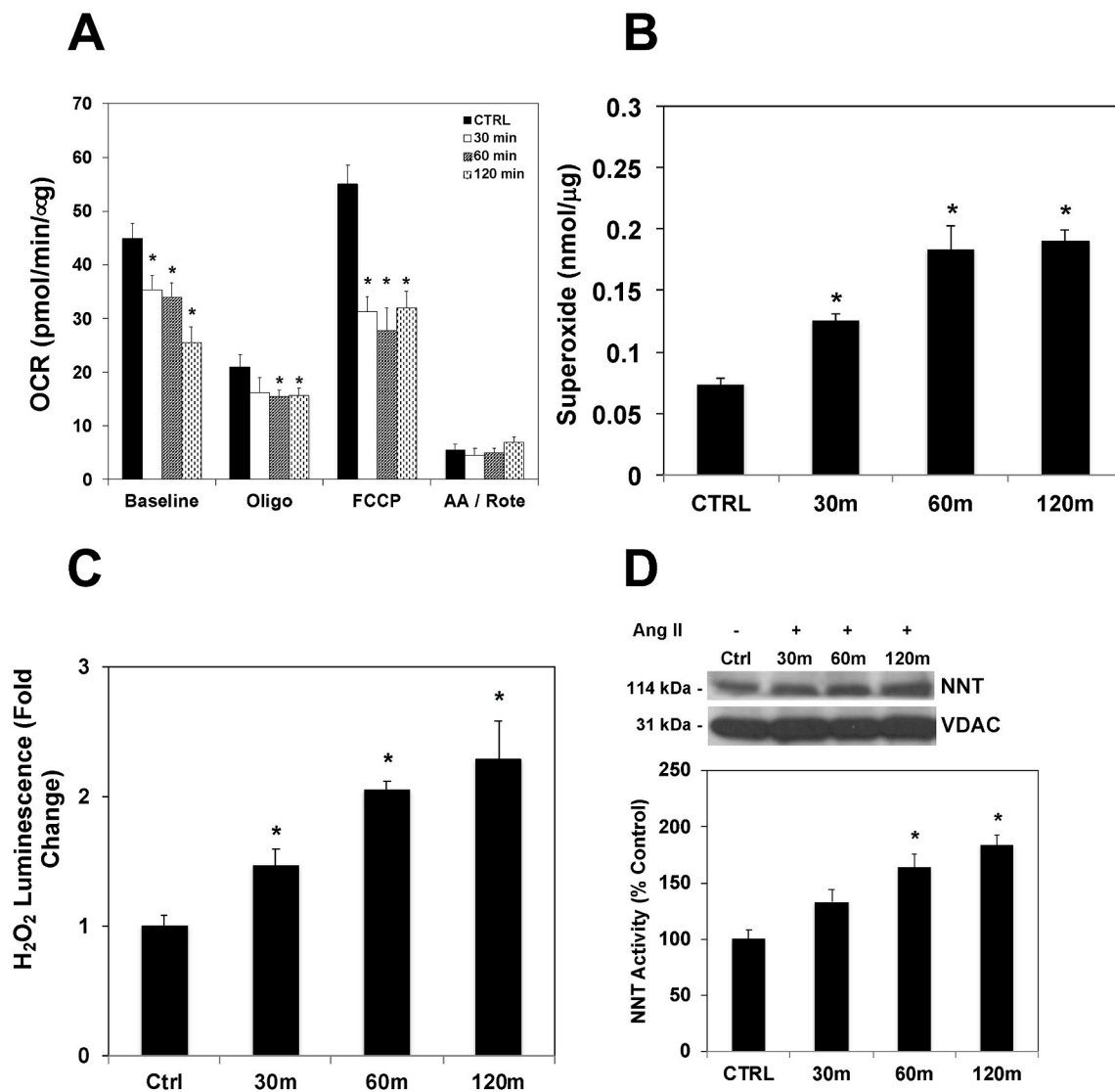
Fig. 1. Ang II promotes mitochondrial dysfunction, ROS production, and NNT expression. Human aortic endothelial cells were treated with Ang II (500 nM) for the times indicated. Mitochondrial function (**A**), superoxide production (**B**), hydrogen peroxide production (**C**), and NNT expression and activity (**D**) was determined. Data presented are means ± SEM of ≥4 independent experiments. *p ≤ 0.05 vs untreated control.

have a significant impact on cellular function as well, since the loss of NNT leads to a marked reduction in ATP levels in these cells (Fig. 3F). These data clearly demonstrate that, in addition to supporting the mitochondrial antioxidant systems, NNT expression and activity is critical to maintaining normal mitochondrial function.

3.4. NNT is required for mitochondrial hyperpolarization in response to Ang II

The ability of the mitochondria to perform its most critical function, the generation of ATP, is dependent on the maintenance of the mitochondrial membrane potential and the proton motive force. NNT also utilizes the mitochondrial membrane potential to convert NADH to NADPH and, as such, the loss of NNT may result in changes to mitochondrial membrane potential. Interestingly, the loss of NNT in HAEC had no impact on mitochondrial membrane potential under unstimulated conditions. However, in cells that contain NNT, Ang II treatment led to time dependent increase in mitochondrial membrane potential that peaked at 30 min of exposure and remained elevated for the duration of the experiment (Fig. 4A and B). Conversely, cells that lack NNT were unable to increase mitochondrial membrane potential in

response to Ang II. The proton motive force generated during oxidative phosphorylation is a critical determinant for the mitochondrial membrane potential and ultimately drives the generation of ATP. Consistent with our observed changes in mitochondrial membrane potential, the loss of NNT had no impact on cellular ATP levels in unstimulated cells (Fig. 3F). However, treatment with Ang II led to a time-dependent increase in ATP levels in Scr cells that was not observed in the absence of NNT (shNNT). These changes in cellular ATP mirror our observations with mitochondrial membrane potential and illustrate the coupling between the mitochondrial membrane potential and ATP production. Furthermore, these data highlight a pivotal role for NNT in regulating mitochondrial function by supporting both stress induced energy production (Fig. 3) and the mitochondrial antioxidant systems (Fig. 2).

3.5. Loss of NNT disrupts Ang II-induced eNOS activity

Previous studies from our laboratory have indicated that the absence of NNT expression led to a more severe hypertensive phenotype in Ang II treated mice [42]. Hypertension was associated with mitochondrial dysfunction, increased vascular ROS production and decreased •NO bioavailability. Our data reveal a similar pattern in NNT knockdown

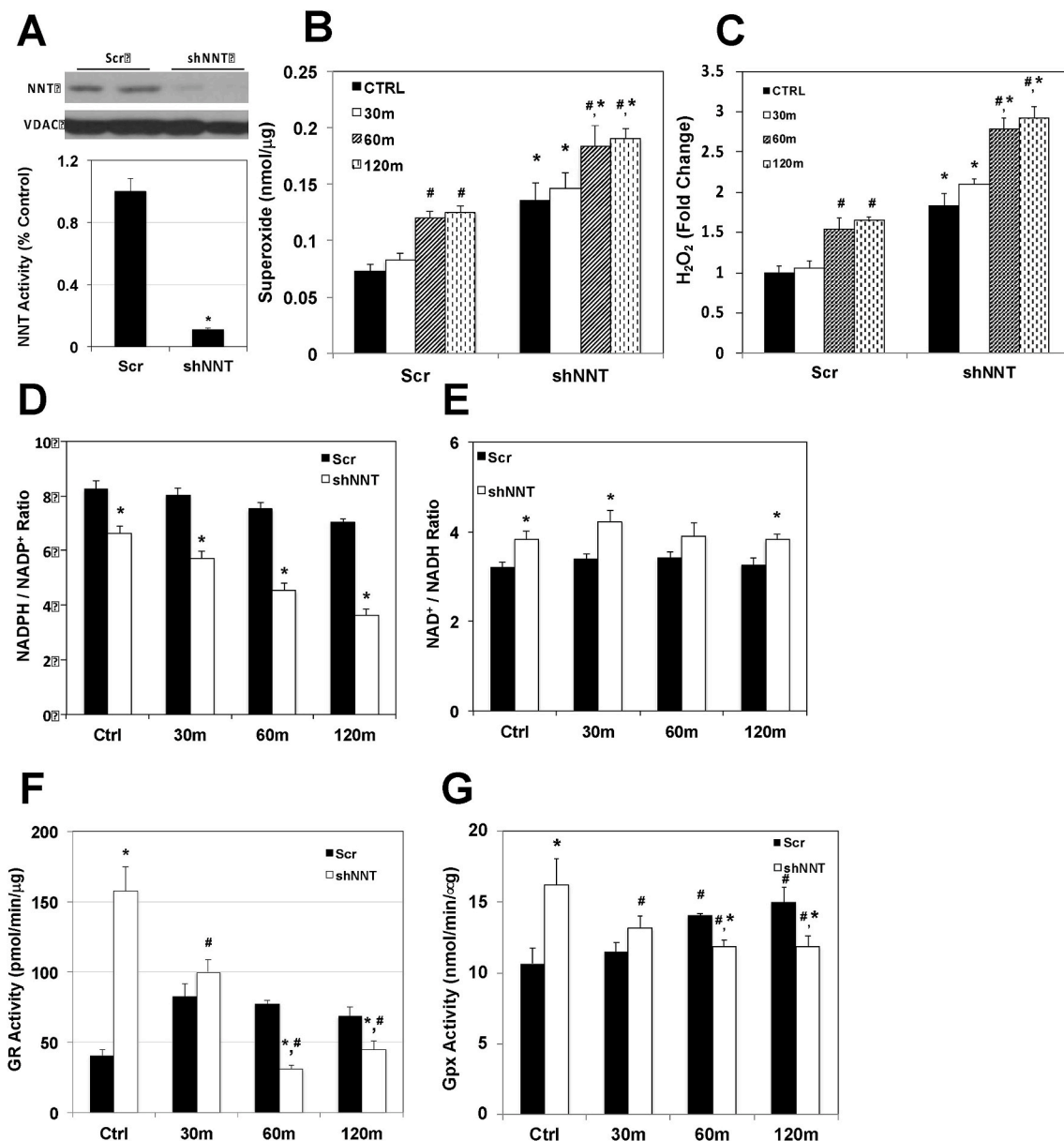**Fig. 2. Knockdown of NNT expression enhances Ang II induced oxidative stress and impairs mitochondrial antioxidant activity.** **(A)** NNT expression and activity following small hairpin RNA knockdown of NNT (shNNT) and scrambled control (Scr) in human aortic endothelial cells (HAEC). Scr and shNNT HAEC were treated with Ang II (500 nM) for the times indicated and mitochondrial superoxide **(B)** and hydrogen peroxide **(C)** were measured. Under similar conditions, NADPH/NADP$^+$ ratios **(D)**, NADH/NAD$^+$ ratios **(E)**, glutathione reductase activity **(F)**, and glutathione peroxidase activity **(G)** were determined. Data presented are means ± SEM of ≥4 independent experiments. *p ≤ 0.05 vs Scr and #p ≤ 0.05 vs untreated control.

HAEC treated with Ang II. To determine if the loss of NNT contributes to a disruption in •NO bioavailability, we assayed eNOS phosphorylation at Ser^{1177} in both Scr and shNNT cells treated with Ang II. As expected, treatment led to a time dependent increase in eNOS phosphorylation in cells with normal NNT expression (Fig. 5A and B). Interestingly, the loss of NNT led to an increase of eNOS phosphorylation at baseline and Ang II treatment exacerbated this effect (Fig. 5A and B). Maximal levels of eNOS phosphorylation was observed at 2 h of Ang II treatment in both groups, with shNNT cells displaying a roughly 2.5 fold increase in phosphorylation compared to Scr. However, increased eNOS phosphorylation in shNNT cells was not associated with an increase in eNOS activity (Fig. 5C). In cells with normal NNT expression, Ang II treatment led to a time-dependent increase in eNOS activity that corresponded with increased eNOS phosphorylation at Ser^{1177}. Conversely, in shNNT cells elevated levels of eNOS phosphorylation at both baseline and following Ang II treatment did not lead to an increase in eNOS activity.

In fact, with 2 and 4 h of Ang II treatment we observed a significant decrease in eNOS activity. Consistent with these observations, cells that contain NNT display a time-dependent increase in •NO production that corresponds with both eNOS phosphorylation and eNOS activity (Fig. 5D). The loss of NNT disrupts this relationship, demonstrating that •NO production parallels the reduction in eNOS activity and not the increased levels of eNOS phosphorylation observed at Ser^{1177}. These data clearly demonstrate that NNT is necessary for the phosphorylation dependent regulation of eNOS activity at Ser^{1177} and the corresponding increase in •NO production. In the absence of NNT, the inability of Ser^{1177} phosphorylation to increase eNOS activity provides valuable mechanistic insight into the decreased •NO bioavailability and exacerbated hypertensive phenotype we have previously observed in C57Bl/6J mice that do not express NNT [42].

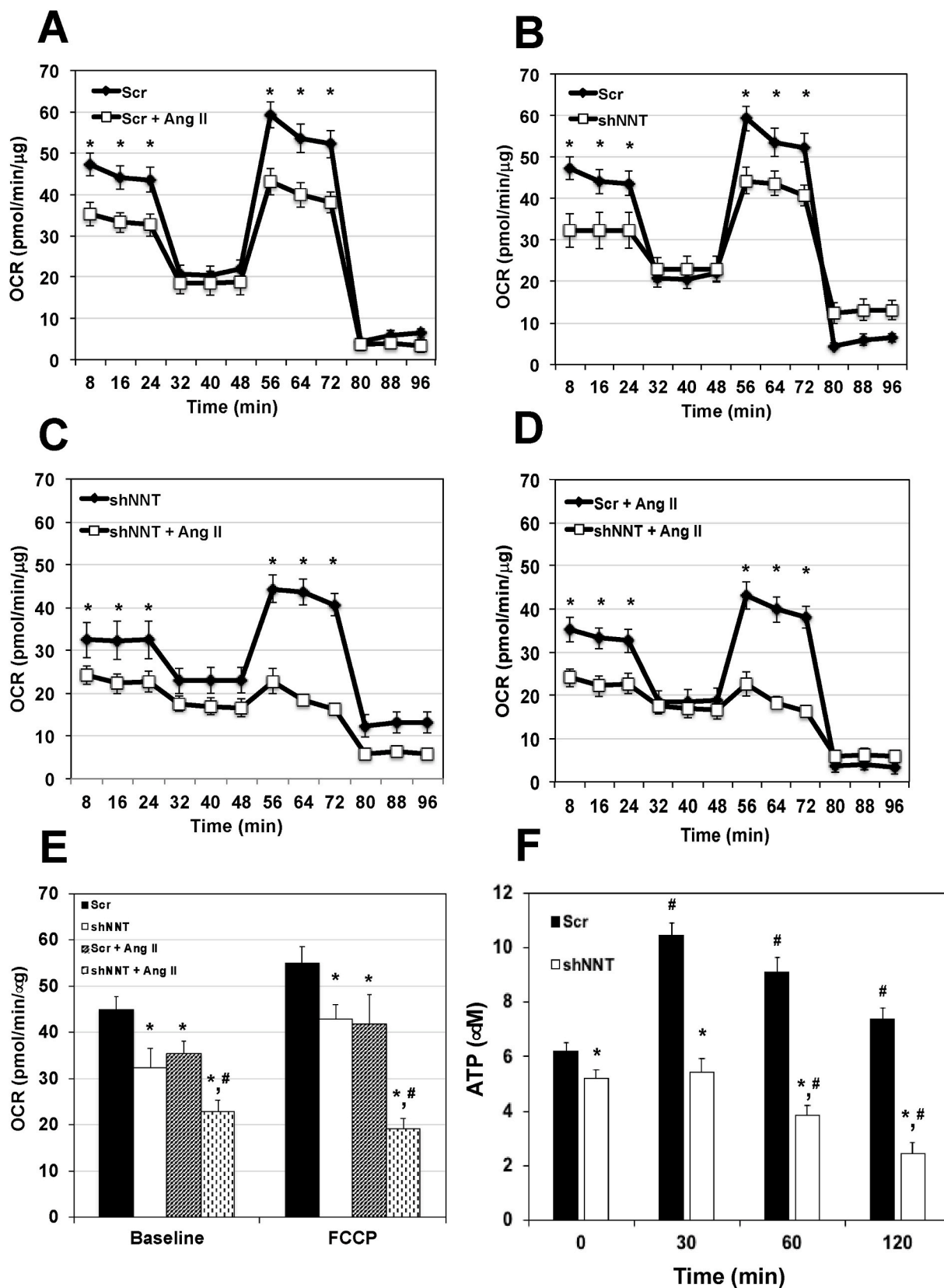**Fig. 3. Knockdown of NNT expression exacerbates mitochondrial dysfunction in response to Ang II.** (**A-D**) Mitochondrial bioenergetic profiles of scrambled and shNNT treated HAEC following exposure to 500 nM Ang II for 2 h. (**E**) Summary data of bioenergetic analysis illustrated in A-D. (**F**) Mitochondrial ATP levels in scrambled and shNNT treated HAEC following exposure to 500 nM Ang II for the times indicated. Values are means ± SEM. of ≥4 independent experiments. A-D *p ≤ 0.05. E and F * p ≤ 0.05 vs Scr and #p ≤ 0.05 vs untreated control.
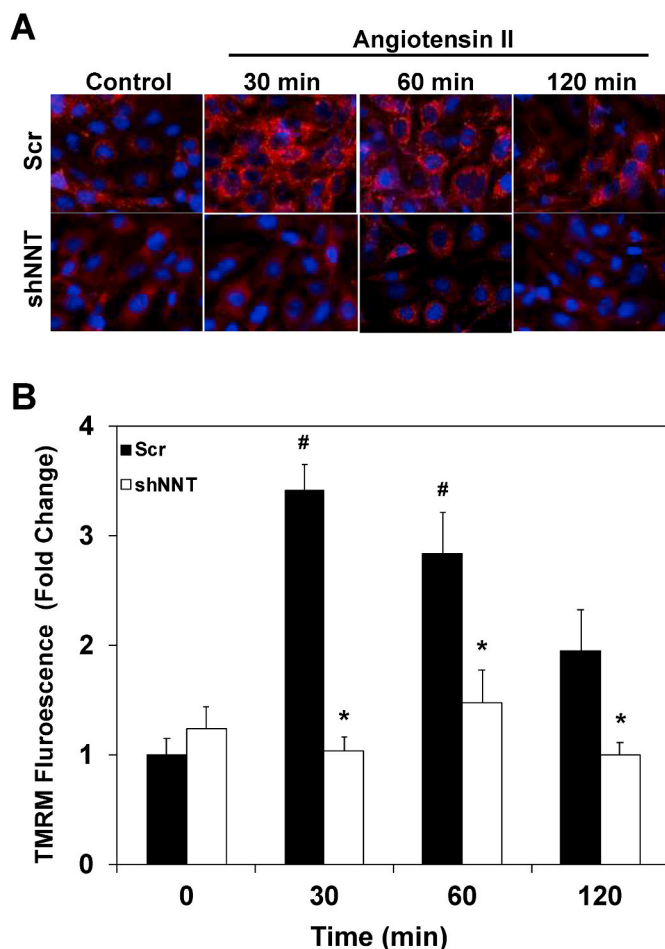
A

Angiotensin II

Control | 30 min | 60 min | 120 min

Scr

shNNT

B

Fig. 4. NNT is required for the dynamic regulation of mitochondrial membrane potential. Scrambled and shNNT treated HAEC were loaded with the potentiometric dye TMRM (50 nM) for 30 min prior to the experiment. Cells were then treated with 500 nM Ang II for the times indicated and mitochondrial membrane potential was determined by live-cell epifluorescent microscopy. Representative images (**A**) and quantitation (**B**) of TMRM fluorescence in response to Ang II. Data presented are means $\pm$ SEM of ≥ 4 independent experiments. *$p \leq 0.05$ vs Scr and #$p \leq 0.05$ vs untreated control.

4. Discussion

Reactive oxygen species (ROS) contribute to changes in vascular tone and the structure of microvasculature contributing to the pathogenesis of HTN [3]. While the NADPH oxidase family of enzymes are a critical source of ROS [3], mounting evidence indicates that mitochondrial-derived ROS may play an equally important role in HTN [4]. Mitochondrial ROS production is counterbalanced by the mitochondrial antioxidant system and NNT is an important source of NADPH in the mitochondria that drives the enzymatic degradation of hydrogen peroxide via peroxidase and reductase systems involving glutathione or thioredoxin as substrates. We have previously shown that C57Bl/6J mice that lack NNT expression have increased levels of vascular ROS production and display a more severe hypertensive phenotype in response to Ang II when compared to C57Bl/6N mice that express NNT [42]. Supporting a role for the endothelium in this process, primary endothelial cells isolated from 6J mice also display mitochondrial dysfunction and increased ROS production [42]. Taken together these observations suggest that NNT expression impacts mitochondrial function and ROS production in response to Ang II that contributes to elevated blood pressure. However, very little is known regarding how NNT expression and activity may impact mitochondrial and endothelial

function in human cells. The current study utilizes normal and shRNA driven NNT knockdown human aortic endothelial cells to determine how NNT expression and activity impacts mitochondrial and endothelial cell function in response to Ang II.

Recent studies indicate that isolated mitochondria from C57Bl/6N mice that contain NNT are reliant on the glutathione and thioredoxin systems to clear exogenously added H_2O_2[50]. However, it is unclear if pathophysiological production of mitochondrial ROS has any impact on the regulation of NNT. In an effort to determine if NNT is regulated by Ang II, we treated human aortic endothelial cells with Ang II and assessed mitochondrial function, ROS production, and NNT expression and activity. Treatment with Ang II led to a time dependent impairment of mitochondrial function (Fig. 1A) characterized by reductions in basal, ATP-linked (oligomycin inhibited), and maximal (FCCP driven) oxygen consumption rates. Consistent with our previous studies, Ang II induced mitochondrial dysfunction was associated with a time dependent increase superoxide and hydrogen peroxide production (Fig. 2B and C). Interestingly, Ang II also let to a time dependent increase in both NNT expression and activity (Fig. 2D). These data are in agreement with previous studies that have shown increased mitochondrial ROS production in endothelial cells treated with Ang II [51–53]. However, this study has, for the first time, demonstrated that Ang II treatment and the associated production of mitochondrial ROS can impact the expression and activity of NNT in human cells. These data are consistent with NNT's role in supporting the mitochondrial antioxidant system and indicate that elevated levels of ROS lead to a compensatory increase in NNT expression and activity to deal with this stress.

While the elevated expression and activity of NNT are consistent with its role in supporting the mitochondrial antioxidant system, we wanted to determine if the targeted removal of this enzyme would have any impact on endothelial redox balance in response to Ang II. Numerous studies, including our own, have utilized the C57Bl/6N and C57Bl/6J mice or cells isolated from them to implicate NNT in regulating mitochondrial redox balance across a wide variety of disease models [33,34,39–42,49]. However, there are strain associated differences in addition to NNT that cannot be adequately accounted for [54–57] and very few studies have specifically looked at NNT in human cells. To investigate how NNT may impact mitochondrial redox balance in human aortic endothelial cells, we generated a stable NNT knockdown cell line using shRNA and compared its responses to a scrambled shRNA line. The shNNT cell line demonstrated a near complete abolishment of both NNT expression and activity (Fig. 2A). Interestingly, simply removing NNT from the mitochondria led to a significant increase in both superoxide and hydrogen peroxide production (Fig. 2B and C). As before, treatment with Ang II incited ROS production, however this response was exacerbated in cells that lack NNT. The observed increases in superoxide and hydrogen peroxide could be due to both increased production and decreased scavenging. We observed no changes in SOD2 expression (data not shown) supporting increased superoxide production during oxidative phosphorylation. Furthermore, elevated superoxide production should drive increases in hydrogen peroxide, as it is the product of superoxide dismutation. These results suggested that an impairment of the mitochondrial antioxidant system supported by NNT's production of NADPH could impact cellular redox balance.

Assessment of the NADPH/NADP$^+$ and NADH/NAD$^+$ ratios demonstrated that the loss of NNT led to a significant decrease in the NADPH/NADP$^+$ ratio and a corresponding increase in the NADH/NAD$^+$ (Fig. 2D &E). We observed no changes in the expression of mitochondrial isocitrate dehydrogenase, malic enzyme or glutamate dehydrogenase (data not shown) as alternative enzymatic sources of NADPH, indicating that there was no compensation for the loss of NNT. The lack of compensation suggests that the reduction of NADPH related to the loss of NNT did not significantly disrupt normal cellular function. The shift in the NADH/NAD$^+$ ratio is consistent with less NADH being consumed by NNT for the production of NADPH. Ang II treatment led to a progressive
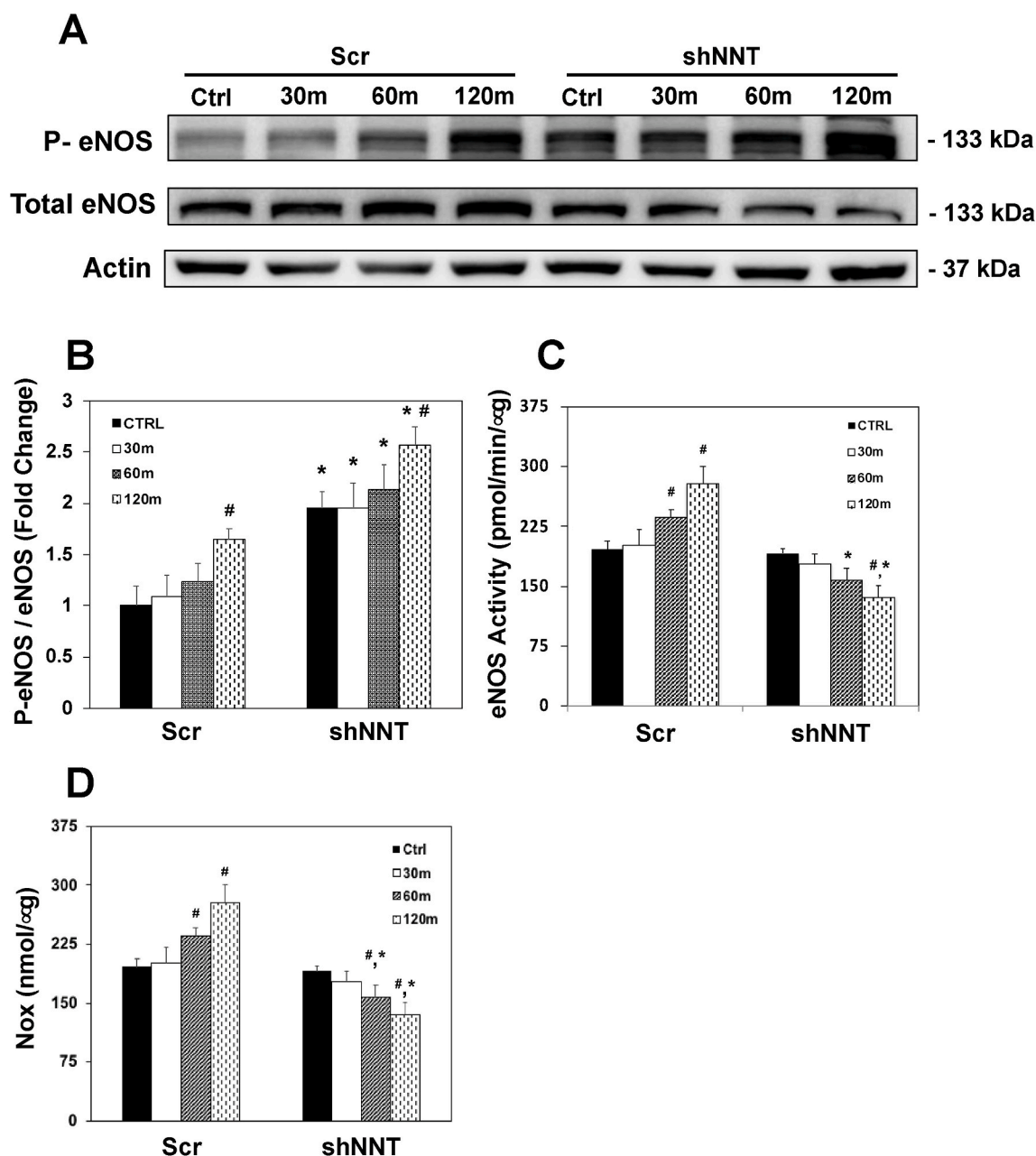
Fig. 5. NNT knockdown disrupts eNOS activity. Scrambled and shNNT treated HAEC were exposed to Ang II (500 nM) for the times indicated and eNOS phosphorylation at Ser[1177] (**A & B**), eNOS activity (**C**), and nitric oxide metabolite (NOx) production (**D**) was determined. Data presented are means ± SEM of ≥4 independent experiments. *p ≤ 0.05 vs Scr and #p ≤ 0.05 vs untreated control.

decrease in the NADPH/NADP$^+$ ratio consistent with NADPH consumption by the mitochondrial antioxidant system. The ability for the loss of NNT to impact cellular NADPH levels is notable. Previous studies have indicated that, under conditions of oxidative stress, that the pentose phosphate pathway can compensate for decreases in NADPH by shifting substrates from glucose metabolism to the pentose phosphate pathway [58]. While analysis of this pathway is beyond the scope of the current study, is possible that activation of this pathway may not be able to entirely compensate for the loss of NADPH resulting from the impaired NNT activity. Examination of glutathione reductase (GR) and glutathione peroxidase (Gpx), components of the mitochondrial antioxidant system that rely on NADPH for their reducing power, indicated that the loss of NNT led to a significant increase in both activities in untreated cells (Fig. 2F &G). While these data initially seemed counterintuitive, they suggest that the loss of NNT and the increased

steady-state levels of ROS present in the mitochondria lead to an increase in GR and Gpx activity to compensate for this stress. While Ang II stimulated GR and Gpx activity in cells that contain NNT, those without had a marked decrease in GR and Gpx activity in response to Ang II. Under these conditions, the elevated levels of ROS production coupled with decreased NADPH production appears to overwhelm the mitochondrial antioxidant system, with GR and Gpx activity dropping as the NADPH is consumed. Taken together, these data demonstrate that the loss of NNT shifts the cellular redox balance, culminating in increased ROS production and impaired thiol-dependent peroxidase and reductase activity.

Mitochondrial dysfunction is a key initiating event that contributes to the endothelial and vascular dysfunction in hypertension. The observed increase in ROS production in untreated cells that lack NNT led to investigations into the relationship between NNT expression and Ang

II-induced mitochondrial dysfunction. Consistent with our parental HAEC line, the Scr cell line that maintains NNT expression displayed significant mitochondrial dysfunction in response to Ang II (Fig. 3A). When comparing untreated Scr and shNNT cells, we observe a similar level of mitochondrial dysfunction through the targeted removal of NNT from these cells (Fig. 3B). Since mitochondrial ROS generation is byproduct of normal energy metabolism, it stands to reason that the loss of NNT and an inhibition of the NADPH dependent antioxidant system in the mitochondria will lead to increased steady state levels of mitochondrial ROS (Fig. 2B and C) contributing to mitochondrial dysfunction. When comparing mitochondrial function in Scr and shNNT cells treated with Ang II, we found that Ang II led to severe mitochondrial dysfunction in cells that lack NNT (Fig. 3D). The results from these experiments suggest that the loss of NNT promotes mitochondrial dysfunction and further sensitizes the mitochondria to Ang II treatment. Furthermore, they provide mechanistic insight into why animals that lack NNT expression often present with a more severe disease phenotype then those that maintain NNT expression [40–42,49,59]. Our data support the concept that the loss of NNT places cells under a mild oxidative stress, or a first hit, that primes them for a severe pathological response when hit with a second pathological stimulus like Ang II. Interestingly, the changes that we observe in the functional properties of the mitochondria did not directly translate to an impairment of energy metabolism. In Scr cells, Ang II treatment led to an early enhancement of mitochondrial ATP production that then diminished over the course of the treatment but did remain significantly elevated when compared to untreated controls (Fig. 3F). This ability to increase ATP production in response to Ang II was lost in shNNT cells, where their mitochondrial ATP progressively decreased in response to treatment. The disconnect between impairment of oxygen consumption rate as an index of oxidative phosphorylation and the production of ATP suggests that NNT may impact other pathways related to energy metabolism. For example, the increased ATP observed in Scr cells treated with Ang II may be related to an impact on the Krebs cycle associated with NNT activity. The production of NADPH by NNT occurs at the expense of NADH and this consumption of NADH may stimulate Krebs cycle activity, and further glycolysis, to replenish NADH stores. As a result, ATP production may occur via other pathways and could explain the elevations in ATP levels we observe despite impairment of oxidative phosphorylation.

The measurement of oxygen consumption provides substantial insight into mitochondrial substrate utilization and electron transfer. However, it is the generation of the mitochondrial membrane potential ($\Delta\Psi$) or the proton motive force that provides the energy for ATP synthesis and has been tightly associated with ATP production [60]. In an effort to determine if NNT impacts mitochondrial membrane potential in response to Ang II, we loaded the mitochondria with TMRM and then treated Scr and shNNT cells with Ang II to track changes in membrane potential. Despite reductions in mitochondrial function and ATP production with the loss of NNT, mitochondrial membrane potential was unaffected in untreated shNNT cells (Fig. 4A and B). However, treatment with Ang II led to markedly different changes in mitochondrial membrane potential in these cells. Consistent with the ATP data, treatment with Ang II let to a significant increase in mitochondrial membrane potential at 30 min that was trending towards baseline by 2 h in the cells that contain NNT. Conversely, shNNT cells displayed little to no change in mitochondrial membrane potential in response to Ang II across any of the treatment time points. The parallels that we observe between mitochondrial membrane potential and ATP production in this system indicates that mitochondrial membrane potential and the proton motive force drive ATP production in these cells. Furthermore, the loss of NNT impairs the ability of these cells to dynamically regulate mitochondrial membrane potential and ATP production in response to Ang II. The ability of NNT to impact the mitochondrial membrane potential is not entirely unexpected since it also uses energy from the mitochondrial membrane potential to perform its transhydrogenase activity [61]. However, we would have predicted that under conditions of oxidative stress that NNT would deplete some of the membrane potential. Our data demonstrates exactly the opposite. While the mechanisms by which the loss of NNT has such a dramatic impact on membrane potential require further investigation, the inability of FCCP to increase oxygen consumption shNNT cells treated with Ang II (Fig. 3E) suggests that the loss of NNT impairs electron transport chain (ETC) function. As a result, electron flow through the chain would slow, promoting electron leak and the partial reduction of oxygen to generate superoxide. This reduced flow would also impair maintenance of the mitochondrial membrane potential and ATP production. These data demonstrate the close relationship between mitochondrial membrane potential and ATP production and highlight NNT as a critical enzyme required to preserve the metabolic plasticity to prevent mitochondrial dysfunction in response to Ang II.

The contribution of mitochondrial ROS production to endothelial dysfunction in hypertension is predominantly centered on the regulation of •NO bioavailability. Mitochondrial ROS can impact blood pressure through disruption of •NO dependent vessel dilation [62–64], through consumption reactions [65], and by promoting eNOS uncoupling leading to further ROS generation [66]. To determine if the loss of NNT contributes to a disruption of •NO biology in response to Ang II, we assessed eNOS phosphorylation at Ser^{1177}, eNOS activity, and the production of •NO metabolites (NOx) in Scr and shNNT cells. As expected, Ang II led to a time dependent increase in eNOS phosphorylation at Ser^{1177} that reached statistical significance at 2 h of treatment in cells that contain NNT. In cells that lack NNT, eNOS phosphorylation was significantly elevated at baseline and Ang II exacerbated this effect at all time points (Fig. 5A and B). However, when eNOS activity was assessed in response to Ang II, we observed a disconnect between eNOS phosphorylation and eNOS activity in the shNNT cells (Fig. 5C). While Scr cells displayed a time dependent increase in eNOS activity that paralleled changes in eNOS phosphorylation, shNNT cells displayed no change in eNOS activity at early time points and a reduction in eNOS activity at later time points despite significant increases in phosphorylation. This same pattern was observed when we measured •NO metabolites as an index of •NO production (Fig. 5D). NNT containing cells were able to elevate •NO production in response to Ang II consistent with eNOS phosphorylation and activity while cells that lack NNT displayed impaired •NO production. Typically, reductions in •NO bioavailability in the context of increased ROS production are thought to be mediated by consumption reactions between superoxide and •NO [67]. However, if this were true in our study we would have expected to see reductions in NOx in the absence of NNT, but not reductions in eNOS activity. Our observed impairment of both eNOS activity and NOx, despite increased eNOS phosphorylation support the conclusion that the increased oxidative stress associated with the loss of NNT may contribute to eNOS uncoupling. While further studies are required confirm eNOS uncoupling in this system, it is consistent with our observations and, since eNOS uncoupling can lead to superoxide production, could contribute to both the elevated production of ROS and decreased NOx we observe in shNNT cells treated with Ang II.

Mounting evidence has implicated mitochondrial ROS as a critical mediator in the development of hypertension. The impact of mitochondrial ROS in this process is exemplified by animal studies where treatment with mitochondria-targeted antioxidants can lead to reduced blood pressure when given systemically [52]. However, clinical trials designed to directly scavenge ROS in hypertension have met with little success [18]. The data presented here support the hypothesis that NNT regulates mitochondrial redox balance and protects against endothelial dysfunction in response to Ang II. This study highlights NNT as an enzyme whose activity impacts the glutathione peroxidase system in the mitochondria supporting antioxidant activity at one of the critical sites of ROS generation in the cell. The potential of NNT to impact multiple antioxidant pathways and promote redox balance in the mitochondria provides support for a shift from simple scavenging to targeted therapeutic strategies for reducing oxidant stress in cardiovascular diseases.

These data support the concept that targeting upstream regulators of existing antioxidant systems may prove to be more effective than treatment with ROS scavengers that display a general lack specificity related to the sites of ROS production.

Declaration of competing interest

The authors have no conflicts of interest to disclose.

Acknowledgements

Appendix A. Supplementary data

Supplementary data to this article can be found online at https://doi.org/10.1016/j.redox.2020.101650.

References

[1] E.J. Benjamin, S.S. Virani, C.W. Callaway, et al., Heart disease and stroke statistics-2018 update: a report from the American heart association, Circulation 137 (2018) e67–e492.

[2] R.M. Carey, S. Sakhuja, D.A. Calhoun, et al., Prevalence of apparent treatment-resistant hypertension in the United States, Hypertension 73 (2019) 424–431.

[3] A.C. Montezano, R.M. Touyz, Oxidative stress, Noxs, and hypertension: experimental evidence and clinical controversies, Ann. Med. 44 (2012) S2–S16.

[4] S.I. Dikalov, Z. Ungvari, Role of mitochondrial oxidative stress in hypertension, Am. J. Physiol. Heart Circ. Physiol. 305 (2013) H1417–H1427.

[5] A. Boveris, Determination of the production of superoxide radicals and hydrogen peroxide in mitochondria, Methods Enzymol. 105 (1984) 429–435.

[6] M.D. Brand, C. Affourtit, T.C. Esteves, et al., Mitochondrial superoxide: production, biological effects, and activation of uncoupling proteins, Free Radical Biol. Med. 37 (2004) 755–767.

[7] B.R. Silva, L. Pernomian, L.M. Bendhack, Contribution of oxidative stress to endothelial dysfunction in hypertension, Front. Physiol. 5 (2012) 441.

[8] E. Schulz, T. Jansen, P. Wenzel, et al., Nitric oxide, tetrahydrobiopterin, oxidative stress, and endothelial dysfunction in hypertension, Antioxidants & Redox Signal. 10 (2008) 1115–1126.

[9] P.C. van den Hoogen, E.J. Feskens, N.J. Nagelkerke, et al., The relation between blood pressure and mortality due to coronary heart disease among men in different parts of the world. Seven Countries Study Research Group, N. Engl. J. Med. 342 (2000) 1–8.

[10] A.M. Zafari, M. Ushio-Fukai, M. Akers, et al., Role of NADH/NADPH oxidase-derived H2O2 in angiotensin II-induced vascular hypertrophy, Hypertension 32 (1998) 488–495.

[11] S. Chrissobolis, S.P. Didion, D.A. Kinzenbaw, et al., Glutathione peroxidase-1 plays a major role in protecting against angiotensin II-induced vascular dysfunction, Hypertension 51 (2008) 872–877.

[12] J.D. Widder, D. Fraccarollo, P. Galuppo, et al., Attenuation of angiotensin II-induced vascular dysfunction and hypertension by overexpression of Thioredoxin 2, Hypertension 54 (2009) 338–344.

[13] A.J. Case, J. Tian, M.C. Zimmerman, Increased mitochondrial superoxide in the brain, but not periphery, sensitizes mice to angiotensin II-mediated hypertension, Redox Biol. 11 (2017) 82–90.

[14] N. Ardanaz, X.P. Yang, M.E. Cifuentes, et al., Lack of Glutathione Peroxidase 1 Accelerates Cardiac-specific Hypertrophy and Dysfunction in Angiotensin II Hypertension, vol. 55, Hypertension, 2010.

[15] ERr Miller, L.J. Appel, T.H. Risby, Effect of dietary patterns on measures of lipid peroxidation: results from a randomized clinical trial, Circulation 98 (1998) 2390–2395.

[16] R. Rodrigo, J. González, F. Paoletto, The role of oxidative stress in the pathophysiology of hypertension, Hypertens. Res.: Off. J. Jpn Soc. Hypertension. 34 (2011) 431–440.

[17] R. Rodrigo, H. Prat, W. Passalacqua, et al., Decrease in oxidative stress through supplementation of vitamins C and E is associated with a reduction in blood pressure in patients with essential hypertension 114, Clinical Science, London, England, 1979, pp. 625–634, 2008.

[18] J. Yoshida, K. Yamamoto, T. Mano, et al., AT1 receptor blocker added to ACE inhibitor provides benefits at advanced stage of hypertensive diastolic heart failure, Hypertension 43 (2004) 686–691.

[19] T. Fukai, M. Ushio-Fukai, Superoxide dismutases: role in redox signaling, vascular function, and diseases, Antioxidants Redox Signal. 15 (2011) 1583–1606.

[20] B. Halliwell, J.M.C. Gutteridge, Free Radicals in Biology and Medicine, Oxford University Press, New York, 2007.

[21] I. Mavelli, A. Rigo, R. Federico, et al., Superoxide dismutase, glutathione peroxidase and catalase in developing rat brain, Biochem. J. 204 (1982) 535–540.

[22] P.C. Engel, Glutamate dehydrogenases: the why and how of coenzyme specificity, Neurochem. Res. 39 (2014) 426–432.

[23] S.H. Jo, M.K. Son, H.J. Koh, et al., Control of mitochondrial redox balance and cellular defense against oxidative damage by mitochondrial NADP+-dependent isocitrate dehydrogenase, J. Biol. Chem. 276 (2001) 16168–16176.

[24] J.A. Ronchi, A. Francisco, L.A. Passos, et al., The contribution of nicotinamide nucleotide transhydrogenase to peroxide detoxification is dependent on the respiratory state and counterbalanced by other sources of NADPH in liver mitochondria, J. Biol. Chem. 291 (2016) 21073–20187.

[25] J. Rydström, N.A.D.P.H. Mitochondrial, transhydrogenase and disease, Biochim. Biophys. Acta 1757 (2006) 721–726.

[26] J.K. Teller, L.A. Fahien, J.W. Davis, Kinetics and regulation of hepatoma mitochondrial NAD(P) malic enzyme, J. Biol. Chem. 267 (1992) 10423–10432.

[27] F. Yin, H. Sancheti, E. Cadenas, Silencing of nicotinamide nucleotide transhydrogenase impairs cellular redox homeostasis and energy metabolism in PC12 cells, Biochim. Biophys. Acta 1817 (2012) 401–409.

[28] S.R. Earle, R.R. Fisher, A direct demonstration of proton translocation coupled to transhydrogenation in reconstituted vesicles, J. Biol. Chem. 255 (1980) 827–830.

[29] T. Olausson, O. Fjellström, J. Meuller, et al., Molecular biology of nicotinamide nucleotide transhydrogenase–a unique proton pump, Biochim. Biophys. Acta 1231 (1995) 1–19.

[30] J. Rydström, A. Teixeira da Cruz, L. Ernster, Factors governing the steady state of the mitochondrial nicotinamide nucleotide transhydrogenase system, Biochem. J. 116 (1970) 12P–13P.

[31] E. Evangelou, H.R. Warren, D. Mosen-Ansorena, et al., Genetic analysis of over 1 million people identifies 535 new loci associated with blood pressure traits, Nat. Genet. 50 (2018) 1412–1425.

[32] Y. Hiura, Y. Tabara, Y. Kokubo, et al., A genome-wide association study of hypertension-related phenotypes in a Japanese population, Circ. J.: Off. J. Jpn. Circu. Soc. 74 (2010) 2353–2359.

[33] H. Freeman, K. Shimomura, E. Horner, et al., Nicotinamide nucleotide transhydrogenase: a key role in insulin secretion, Cell Metabol. 3 (2006) 35–45.

[34] T.T. Huang, M. Naeemuddin, S. Elchuri, et al., Genetic modifiers of the phenotype of mice deficient in mitochondrial superoxide dismutase, Hum. Mol. Genet. 15 (2006) 1187–1194.

[35] J.A. Ronchi, T.R. Figueira, F.G. Ravagnani, et al., A spontaneous mutation in the nicotinamide nucleotide transhydrogenase gene of C57BL/6J mice results in mitochondrial redox abnormalities, Free Radical Biol. Med. 63 (2013) 446–456.

[36] K.H. Fisher-Wellman, T.E. Ryan, C.D. Smith, et al., A direct comparison of metabolic responses to high-fat diet in C57BL/6J and C57BL/6NJ mice, Diabetes 65 (2016) 3249–3261.

[37] N. Wong, A.R. Blair, G. Morahan, et al., The deletion variant of nicotinamide nucleotide transhydrogenase (Nnt) does not affect insulin secretion or glucose tolerance, Endocrinology 151 (2010) 96–102.

[38] A.G. Nickel, A. von Hardenberg, M. Hohl, et al., Reversal of mitochondrial transhydrogenase causes oxidative stress in heart failure, Cell Metabol. 22 (2015) 472–484.

[39] K. Kaku, F.T.J. Fiedorek, M. Province, et al., Genetic analysis of glucose tolerance in inbred mouse strains. Evidence for polygenic control, Diabetes 37 (1988) 707–713.

[40] R.S. Surwit, C.M. Kuhn, C. Cochrane, et al., Diet-induced type II diabetes in C57BL/6J mice, Diabetes 37 (1988) 1163–1167.

[41] R.S. Surwit, M.F. Seldin, C.M. Kuhn, et al., Control of expression of insulin resistance and hyperglycemia by different genetic factors in diabetic C57BL/6J mice, Diabetes 40 (1991) 82–87.

[42] I. Leskov, A. Neville, X. Shen, et al., Nicotinamide nucleotide transhydrogenase activity impacts mitochondrial redox balance and the development of hypertension in mice, J. Am. Soc. Hypertens. S1933–1711 (2016) 30601–30605.

[43] F.L. Sheeran, J. Rydström, M.I. Shakhparonov, et al., Diminished NADPH transhydrogenase activity and mitochondrial redox regulation in human failing myocardium, Biochemica et Biophysica Acta 1797 (2010) 1138–1148.

[44] M. Yamaguchi, Youssef Hatefi, Mitochondrial energy-linked nicotinamide nucleotide transhydrogenase. Membrane topography of the bovine enzyme, J. Biol. Chem. 266 (1991) 5728–5735.

[45] D.A. Ferrick, A. Neilson, C. Beeson, Advances in measuring cellular bioenergetics using extracellular flux, Drug Discov. Today 13 (2008) 268–274.

[46] A.A. Gerencser, A. Neilson, S.W. Choi, et al., Quantitative microplate-based respirometry with correction for oxygen diffusion, Anal. Chem. 81 (2009) 6868–6878.

[47] J. Zielonka, J. Vasquez-Vivar, B. Kalyanaraman, Detection of 2-hydroxyethidium in cellular systems: a unique marker product of superoxide and hydroethidine, Nat. Protoc. 3 (2008) 8–21.

[48] G.K. Kolluru, S. Yuan, X. Shen, et al., H2S regulation of nitric oxide metabolism, Methods Enzymol. 554 (2015) 271–297.

[49] A.E. Vozenilek, M. Vetkoetter, J.M. Green, et al., Absence of nicotinamide nucleotide transhydrogenase in C57BL/6J mice exacerbates experimental atherosclerosis, J. Vasc. Res. 55 (2018) 98–110.

[50] I. Dogar, S. Dixon, R. Gill, et al., C57BL/6J mice upregulate catalase to maintain the hydrogen peroxide buffering capacity of liver mitochondria, Free Radical Biol. Med. 146 (2020) 59–69.

[51] S.I. Dikalov, R.R. Nazarewicz, A. Bikineyeva, et al., Nox2-induced production of mitochondrial superoxide in angiotensin II-mediated endothelial oxidative stress and hypertension, Antioxidants & Redox Signal. 20 (2014) 281–294.

[52] A.E. Dikalova, A.T. Bikineyeva, K. Budzyn, et al., Therapeutic targeting of mitochondrial superoxide in hypertension, Circ. Res. 107 (2010) 106–116.

[53] A.K. Doughan, D.G. Harrison, S.I. Dikalov, Molecular mechanisms of angiotensin II-mediated mitochondrial dysfunction: linking mitochondrial oxidative damage and vascular endothelial dysfunction, Circ. Res. 102 (2008) 488–496.

[54] C. Attané, M.L. Peyot, R. Lussier, et al., Differential insulin secretion of high-fat diet-fed C57BL/6NN and C57BL/6NJ mice: implications of mixed genetic background in metabolic studies, PloS One 11 (2016), e0159165.

[55] D.A. Fontaine, D.B. Davis, Attention to background strain is essential for metabolic research: C57BL/6 and the international knockout mouse consortium, Diabetes (2016) 1.

[56] J.T. Heiker, A. Kunath, J. Kosacka, et al., Identification of genetic loci associated with different responses to high-fat diet-induced obesity in C57BL/6N and C57BL/6J substrains, Physiol. Genom. 46 (2014) 377–384.

[57] K. Mekada, K. Abe, A. Murakami, et al., Genetic differences among C57BL/6 substrains, Exp. Anim. 58 (2009) 141–149.

[58] D. Peralta, A.K. Bronowska, B. Morgan, et al., A proton relay enhances H2O2 sensitivity of GAPDH to facilitate metabolic adaptation, Nat. Chem. Biol. 11 (2015) 156–163.

[59] A. Nicholson, P.C. Reifsnyder, R.D. Malcolm, et al., Diet-induced obesity in two C57BL/6 substrains with intact or mutant nicotinamide nucleotide transhydrogenase (Nnt) gene, Obesity 18 (2010) 1902–1905.

[60] L.D. Zorova, V.A. Popkov, E.Y. Plotnikov, et al., Mitochondrial membrane potential, Annal. Biochem. 552 (2018) 50–59.

[61] D. Kampjut, L.A. Sazanov, Structure and mechanism of mitochondrial proton-translocating transhydrogenase, Nature 573 (2019) 291–295.

[62] R.A. Cohen, T. Adachi, Nitric-oxide-induced vasodilatation: regulation by physiologic s-glutathiolation and pathologic oxidation of the sarcoplasmic endoplasmic reticulum calcium ATPase, Trends Cardiovasc. Med. 16 (2006) 109–114.

[63] A. Takaki, K. Morikawa, M. Tsutsui, et al., Crucial role of nitric oxide synthases system in endothelium-dependent hyperpolarization in mice, J. Exp. Med. 205 (2008) 2053–2063.

[64] M.S. Wolin, S.A. Gupte, B.H. Neo, et al., Oxidant-redox regulation of pulmonary vascular responses to hypoxia and nitric oxide-cGMP signaling, Cardiol. Rev. 18 (2010) 89–93.

[65] B.A. Freeman, C.R. White, H. Gutierrez, et al., Oxygen radical-nitric oxide reactions in vascular diseases, Adv. Pharmacol. 34 (1995) 45–69.

[66] T. Münzel, A. Daiber, V. Ullrich, et al., Vascular consequences of endothelial nitric oxide synthase uncoupling for the activity and expression of the soluble guanylyl cyclase and the cGMP-dependent protein kinase, Arterioscler. Thromb. Vasc. Biol. 25 (2005) 1551–1557.

[67] Q. Li, J.Y. Youn, H. Cai, Mechanisms and consequences of endothelial nitric oxide synthase dysfunction in hypertension, J. Hypertens. 33 (2015) 1128–1136.